

Scaling and interleaving of sub-system Lyapunov exponents for spatio-temporal systems

R. Carretero-González^{‡,*}, S. Ørstavik[‡], J. Huke[‡], D.S. Broomhead[‡] and J. Stark[‡]

[‡]Centre for Nonlinear Dynamics and its Applications[†], University College London, Gower Street, London WC1E 6BT, U.K.

[‡]Department of Mathematics, University of Manchester Institute of Science & Technology, Manchester M60 1QD, U.K.

(October 13, 2018, Submitted to *Chaos*, August 1998)

The computation of the entire Lyapunov spectrum for extended dynamical systems is a very time consuming task. If the system is in a chaotic spatio-temporal regime it is possible to approximately reconstruct the Lyapunov spectrum from the spectrum of a sub-system in a very cost effective way. In this work we present a new rescaling method, which gives a significantly better fit to the original Lyapunov spectrum. It is inspired by the stability analysis of the homogeneous evolution in a one-dimensional coupled map lattice but appears to be equally valid in a much wider range of cases. We evaluate the performance of our rescaling method by comparing it to the conventional rescaling (dividing by the relative sub-system volume) for one and two-dimensional lattices in spatio-temporal chaotic regimes. In doing so we notice that the Lyapunov spectra for consecutive sub-system sizes are interleaved and we discuss the possible ways in which this may arise. Finally, we use the new rescaling to approximate quantities derived from the Lyapunov spectrum (largest Lyapunov exponent, Lyapunov dimension and Kolmogorov-Sinai entropy) finding better convergence as the sub-system size is increased than with conventional rescaling.

CONTENTS

I	Introduction	1
II	One-dimensional coupled map lattices	3
	A Interleaving and rescaling for homogeneous states	3
	B Interleaving and rescaling for coupled logistic maps	6
	C Estimation of quantities derived from the Lyapunov spectrum	10
III	More general extended dynamical systems	11
	A Chaotic neural networks	11
	B Two-dimensional logistic lattice	12
	C Host-parasitoid system	14
IV	Conclusions	16

I. INTRODUCTION

Spatio-temporal systems give rise to a wide range of interesting phenomena that cannot occur in dynamical systems with only a few degrees of freedom. The most common approach to modelling complex spatio-temporal behaviour is through the use of partial differential equations (PDE's). The analysis and even the numerical integration of PDE's is usually quite intricate. Thus, if one desires to study the full range of complex spatio-temporal behaviour whilst conserving a relatively simple dynamical framework, a better approach is to consider discrete spatio-temporal systems. By this we mean a collection of coupled simple low-dimensional dynamical units arranged on a spatial lattice. The coupling is usually (but not always) restricted to a finite neighbourhood. An immediate advantage of such systems is their straightforward computational implementation. Another possible advantage is that the local dynamics at each lattice site in the uncoupled limit can be thoroughly analysed. The knowledge of such local dynamics in the uncoupled limit can help to provide some insight of the complexity of the coupled system.

In this paper we are particularly interested in the characterization of chaos in such extended dynamical systems. The most basic tool for analyzing a chaotic system is its Lyapunov exponents. The Lyapunov exponents are an important invariant of nonlinear dynamical systems and are closely related to other quantities of interest. Consider a discrete spatio-temporal system with N state variables where N is the number of local variables times the spatial volume of the system, for example $N = \eta L^d$ for a d -dimensional cubic lattice of side L with η variables in each node. For such an N -dimensional system there exist N Lyapunov exponents corresponding to the rates of expansion and/or contraction of nearby orbits in the tangent space in each dimension. The *Lyapunov spectrum* (LS) is defined as the set $\{\lambda_i\}_{i=1}^N$ of the N Lyapunov exponents arranged in decreasing order. The LS is very useful in the characterization of a chaotic attractor since it gives an estimate of its dimension by means of the *Lyapunov dimension* D_L (Kaplan-Yorke conjecture [1,2]) defined as

$$D_L = j + \frac{1}{\lambda_{j+1}} \sum_{i=1}^j \lambda_i, \quad (1)$$

where j is the largest integer for which $\sum_{i=1}^j \lambda_i > 0$. Another useful invariant that can be derived from the

*e-mail: R.Carretero@ucl.ac.uk

[†]<http://www.ucl.ac.uk/CNDA>

LS is the so called *Kolmogorov-Sinai* (KS) entropy h that can be bounded from above by the sum of the positive Lyapunov exponents λ_i^+ and that in many cases can be well approximated by [3]

$$h = \sum \lambda_i^+. \quad (2)$$

The KS entropy quantifies the mean rate of information production in a system, or alternatively the mean rate of growth of uncertainty in a system subjected to small perturbations.

When dealing with extended dynamical systems, the high number of variables, and even the number of effective degrees of freedom, often leads to severe difficulties because of the large amount of resources (computing time and memory space) required for many computations. Therefore it is useful, and often crucial, to develop techniques that derive information about the whole system by analyzing a comparatively small sub-system. For dynamical systems with only a few degrees of freedom the computation of the LS is a straightforward task; however, when the number of degrees of freedom gets large (*e.g.* a few hundred) it becomes a painstaking process [4–6]. In particular, any algorithm to compute the LS must contain two fundamental procedures; one to multiply by the Jacobian at each time step and the other to perform some kind of reorthogonalization [7]. The latter is required to prevent the Jacobian matrix progressively getting more ill-conditioned, until the largest Lyapunov exponent swamps all the others. Such orthogonalization procedures are based upon the factorization of the Jacobian matrix into a product of an orthogonal matrix Q and an upper triangular matrix R . The two most widespread methods for achieving such orthogonalization are based upon modified Gram-Schmidt (MGS) orthogonalization and the so-called HQR decomposition that uses Householder transformations. The MGS-based methods are widely used because of their quite simple numerical implementation though they are known to introduce small errors due to the fact that the orthogonality of the matrix Q may fail. The HQR-based methods are more difficult to implement but they give a better approximation of the LS [8] since they do not have the problem of losing orthogonality of the matrix Q . The difficulty in using any of these methods for computing the LS of systems with a high number of degrees of freedom N is that they require $\mathcal{O}(N^3)$ operations [8]. The usual naive algorithm for matrix multiplication is also $\mathcal{O}(N^3)$, so that overall computing the full LS is an $\mathcal{O}(N^3)$ process (in principle matrix multiplication can be done faster than $\mathcal{O}(N^3)$ using specialized techniques, but this hardly seems worth doing under the circumstances). As an example, the computation of the LS using a HQR method for a logistic coupled map lattice with $N = 100$ takes a few hours on a standard workstation. When the system size is an order of magnitude larger (*e.g.* for two or more spatial dimensions) and/or the convergence of the Lyapunov exponents is rather slow, the task quickly becomes infeasible. Therefore one must rely on other techniques

to approximate the LS for large systems.

One such technique to estimate the LS in a fully spatio-temporal chaotic regime is to take a principal sub-matrix of the Jacobian and compute the LS for this sub-system. It has been observed in a wide range of spatio-temporal systems that such a sub-system LS converges to the spectrum of the whole system under appropriate rescaling. In a number of specialized cases *e.g.* turbulent Navier-Stokes flows [9] and hard sphere gases [11,10] there are rigorous results for this phenomenon. However it seems difficult to prove its occurrence more generally, and certainly there are many systems where it is observed numerically but no rigorous analysis exists. These include coupled logistic maps [4], chaotic neural networks [12], coupled map lattices [13,14], reaction-diffusion systems [15,16] (lattice of ODEs), turbulent fluids [17], the Kuramoto-Sivashinsky model [18] (PDE's), and others.

Such a rescaling approach consists of evolving the *whole* N -dimensional system under the equations of motion, taking a *sub-system* of size N_s to compute the LS and then rescaling it to obtain an estimate of the original LS. This method relies on the linear increase of Lyapunov dimension D_L and KS entropy h with the sub-system size (see above references). A physical interpretation of this phenomenon can be given in terms of the thermodynamic limit of the system. A spatio-temporal system in a fully chaotic regime will possess a typical correlation length ξ such that elements further apart than ξ evolve almost independently from each other. The whole system can then be thought of in some sense as the union of several almost independent sub-systems of size ξ . In the limit when these sub-systems are completely uncoupled the LS repeats itself in each one of them. If an interaction between the sub-systems is introduced, one may expect the overall LS not to be significantly altered. Thus in the limit of a large number of degrees of freedom, a number of Lyapunov exponents per ξ -volume may be defined. One expects such an intuitive picture to become more accurate in the limit of a large number of degrees of freedom and a small correlation length.

When examining closer the Lyapunov spectra in the fully chaotic regime for several spatio-temporal systems we found that the Lyapunov exponents of two consecutive sub-system sizes N_s and $N_s + 1$ were interleaved. In other words, the i th Lyapunov exponent for the sub-system N_s lies between the i th and $(i + 1)$ th Lyapunov exponents of the sub-system $N_s + 1$. The interleaving of the eigenvalues for a single matrix is a well-known fact (Cauchy's interlace theorem) and is common in many areas such as Sturm sequences of polynomials [19]. Unfortunately there appears to be no obvious generalization which would imply the same fact for sub-system Lyapunov Spectra.

This paper is organized as follows. In order to study interleaving we begin by examining the properties of sub-system LS in coupled map lattices in section II. In section II A we investigate the simplest case of homoge-

neous evolution where we are able to prove rigorously that interleaving and rescaling occur. This example also suggests a different rescaling of the sub-system LS that is superior to that hitherto used in the literature. In section II B we study the interleaving and rescaling properties of the sub-system LS in the fully chaotic regime for a coupled map lattice. Applying the new rescaling obtained from the homogeneous case turns out to lead to a much better fit to the whole LS. In section II C we show that by using this rescaling it is possible to extrapolate the whole LS and extract better estimates for the largest Lyapunov exponent, the Lyapunov dimension and the KS entropy. In section III we examine the interleaving and rescaling for more complex spatio-temporal systems. We notice that the interleaving is not always exact but the proportion of Lyapunov exponents that do not interleave is very small. We also present some results for two-dimensional systems and point out that one needs to be careful about the choice of sub-system variables. Finally, in section IV we give a brief recapitulation of the results together with a discussion on the applicability of interleaving and rescaling to more general extended dynamical systems.

II. ONE-DIMENSIONAL COUPLED MAP LATTICES

Coupled map lattices [20,21] (CML's) are a popular choice for the study of fully-developed turbulence and pattern formation. The appeal of CML's is due on one hand to their computational simplicity and on the other to the fact that they display a wide variety of spatio-temporal phenomena ranging from spatio-temporal periodic states [22,23] and travelling interfaces [24,25] to intermittency [26] and turbulence [27,28]. A CML is a discrete space-time dynamical system with a continuous state space, in contrast to cellular automata where the state space is discrete. Let us denote by x_i^n the state of the i th site at time n , where the integer index i runs from 1 to N . The CML dynamics is defined by

$$x_i^{n+1} = (1 - \varepsilon)f(x_i^n) + \sum_{k=-l}^r \varepsilon_k f(x_{i+k}^n), \quad (3)$$

where we use periodic boundary conditions, f is a real function and we ask $\sum \varepsilon_k = \varepsilon$ as a conservation law. The general CML (3) couples $l \geq 0$ left neighbours and $r \geq 0$ right neighbours with coefficients ε_k .

A. Interleaving and rescaling for homogeneous states

In order to gain some insight into interleaving and rescaling behaviour of the Lyapunov spectrum in extended dynamical systems let us start with the simplest

case of all: homogeneous evolution. We define *homogeneous states* as states of the form $X_n = \{x_i^n\}_{i=1}^N$ where $x_i^n = x^n$ is the same for all i . It is trivial that by setting the initial state of the lattice to a homogeneous state $x_i^0 = x^0$ one has that $X_n = \{f^n(x^0)\}$ for all i at any future time n . In other words the homogeneity of the initial state is preserved under iteration by (3).

Let us take a simple form for the coupling by using the most widespread model of a CML, the so called *diffusive* CML:

$$x_i^{n+1} = (1 - \varepsilon)f(x_i^n) + \frac{\varepsilon}{2} (f(x_{i-1}^n) + f(x_{i+1}^n)), \quad (4)$$

where now the coupling is symmetric and only between nearest neighbours. We shall perform a linear stability analysis of homogeneous states in this system. Such an analysis for more general CML's has also served as the starting point for the study of signal propagation [29] and pattern formation [22]. Since (4) preserves homogeneity under iteration it is natural to ask whether the stability of f completely determines the stability of the homogeneous state. The answer turns out to be yes.

The Lyapunov exponents λ_i are given by the logarithms of the eigenvalues of the matrix

$$\Gamma = \lim_{n \rightarrow \infty} [P(n)^{\text{tr}} \cdot P(n)]^{1/2n} \quad (5)$$

where

$$P(n) = J(n) \cdot J(n-1) \cdots J(2) \cdot J(1)$$

and where $J(s)$ is the Jacobian matrix of the CML dynamics at time s and $(\cdot)^{\text{tr}}$ denotes matrix transpose. The existence of the limit in equation (5) for almost every orbit (with respect to an ergodic invariant measure) is guaranteed by the multiplicative ergodic theorem [30]. For the homogeneous lattice

$$J(n) = \mu_n \cdot M \quad (6)$$

where $\mu_n = f'(x^n)$ is the multiplier of the local map and M is the constant matrix

$$M = \begin{pmatrix} 1 - \varepsilon & \varepsilon/2 & 0 & \cdots & \varepsilon/2 \\ \varepsilon/2 & 1 - \varepsilon & \varepsilon/2 & \cdots & 0 \\ 0 & \varepsilon/2 & 1 - \varepsilon & \cdots & 0 \\ \vdots & \ddots & \ddots & \ddots & \vdots \\ \varepsilon/2 & \cdots & 0 & \varepsilon/2 & 1 - \varepsilon \end{pmatrix}.$$

The matrix M is not only symmetric but also *circulant*. Recall that a matrix is circulant if in each successive row the elements move to the right one position (with wrap-around at the edges) [31]. It is straightforward to prove [32] that the eigenvalues of a circulant matrix

$$C = \begin{pmatrix} c_0 & c_1 & \cdots & c_{k-1} \\ c_{k-1} & c_0 & \cdots & c_{k-2} \\ \vdots & \ddots & \ddots & \vdots \\ c_1 & c_2 & \cdots & c_0 \end{pmatrix}$$

are given by $c_0 + c_1 r_j + \dots + c_{k-1} r_j^{k-1}$, where $r_j = \exp(2\pi i j/N)$ is an N th root of unity. Thus, the eigenvalues $\beta_j(n)$ of $J(n)$ are given by

$$\begin{aligned}\beta_j(n) &= \mu_n \left((1 - \varepsilon) + \frac{\varepsilon}{2} (r_j + r_j^{N-1}) \right) \\ &= \mu_n \phi_j(\varepsilon, N),\end{aligned}$$

where

$$\phi_j(\varepsilon, N) = (1 - \varepsilon) + \varepsilon \cos\left(\frac{2\pi j}{N}\right). \quad (7)$$

It is important to notice that $\phi_j(\varepsilon, N)$ does not depend on the iteration n : the time dependence has been decoupled (factorized) into μ_n . The Lyapunov exponents are then given by

$$\begin{aligned}\lambda_i &= \lim_{t \rightarrow \infty} \ln \prod_{n=1}^t |\beta_i(n)|^{1/t} \\ &= \lim_{t \rightarrow \infty} \ln \left(|\phi_i(\varepsilon, N)| \prod_{n=1}^t |\mu_n|^{1/t} \right) \\ &= \ln |\phi_i(\varepsilon, N)| + \lim_{t \rightarrow \infty} \frac{1}{t} \sum_{n=1}^t \ln |\mu_n|.\end{aligned}$$

Thus by defining λ_0 to be the Lyapunov exponent of a typical orbit of a single, uncoupled, local map, starting at x^0 : $\lambda_0 = \lim_{t \rightarrow \infty} (1/t) \sum_{n=1}^t \ln |\mu_n|$, one obtains the following expression for the Lyapunov exponents of a homogeneous evolution:

$$\lambda_i = \lambda_0 + \ln |\phi_i(\varepsilon, N)|. \quad (8)$$

Note that the Lyapunov exponents defined by (8) are not arranged in decreasing order. Re-indexing them in decreasing order they become

$$\lambda_k = \begin{cases} \lambda_0 + \ln |\phi_{\frac{k}{2}}(\varepsilon, N)| & k \text{ even} \\ \lambda_0 + \ln |\phi_{\frac{k-1}{2}}(\varepsilon, N)| & k \text{ odd} \end{cases} \quad (9)$$

where $k = 1$ to N . It is clear that $\lambda_k = \lambda_{k+1}$ when k is even, so most of the exponents occur in degenerate pairs, apart from the largest, and, if N is even, the smallest. The linear stability of a homogeneous orbit is then characterized by the Lyapunov exponent λ_0 of a single site in the uncoupled case ($\varepsilon = 0$). In particular, if the local map is not chaotic then the homogeneous evolution is not chaotic either since $\lambda_k \leq \lambda_0$ ($|\phi_k(\varepsilon, N)| \leq 1$ for all k).

It is interesting to notice that the same shape for the LS of a homogeneous CML (*cf.* (8)) is obtained for a lattice of coupled Bernoulli shifts [33] for *any* orbit. There is however an important difference: while in the CML the LS dependence on the actual orbit was decoupled thanks to the homogeneity, in the case of coupled Bernoulli shifts, the LS is decoupled from the orbit because the

derivative of the local map at any point is constant. Examining further this similarity, if one takes the fully chaotic logistic map ($4x(1-x)$) as the local map for the diffusive CML, the LS for the homogeneous evolution is

$$\lambda_i = \ln 2 + \ln |\phi_i(\varepsilon, N)|. \quad (10)$$

In fact, any one-dimensional map whose Lyapunov exponent is $\lambda_0 = \ln 2$ gives rise to the LS (10) under homogeneous evolution. The LS (10) corresponds exactly to the LS of a lattice of coupled Bernoulli shifts and thus the results described below for the rescaling of the sub-system LS are valid for the case of a lattice of coupled Bernoulli shifts.

Now let us perform the LS analysis for a sub-system of the original CML. Thus instead of taking all the sites $i = 1, \dots, N$ we take N_s sites starting at any position j . The choice of j is not important since we are dealing with periodic boundary conditions and because the state is homogeneous; from now on we choose $j = 1$. Thus, we take a principal sub-matrix J' of size $N_s \times N_s$ from the whole Jacobian J . In matrix terms $J' = \pi(J)$ where π is the following projection

$$\pi(J) = \Pi_l \cdot J \cdot \Pi_r \quad (11)$$

with the left (Π_l) and right (Π_r) projection matrices defined as

$$\begin{aligned}\Pi_l &= \left(I \middle| Z \right) \\ \Pi_r &= \left(\begin{array}{c} I \\ Z^{\text{tr}} \end{array} \right)\end{aligned}$$

where, from now on, I is the $N_s \times N_s$ identity matrix and Z is the $N_s \times (N - N_s)$ null matrix. Therefore, in order to compute the Lyapunov exponents for the truncated system one has to compute the following product of projected matrices

$$\begin{aligned}P'(n) &= (\Pi_l J(n) \Pi_r) \cdots (\Pi_l J(2) \Pi_r) (\Pi_l J(1) \Pi_r) \\ &= \Pi_l J(n) \Pi_c J(n-1) \cdots J(2) \Pi_c J(1) \Pi_r,\end{aligned} \quad (12)$$

where

$$\Pi_c = \Pi_r \cdot \Pi_l = \left(\begin{array}{c|c} I & Z \\ \hline Z^{\text{tr}} & 0 \end{array} \right).$$

Multiplying equation (12) from the left by the identity matrix obtained by $\Pi_l \cdot \Pi_r = I$ yields

$$\begin{aligned}P'(n) &= \Pi_l \Pi_r \Pi_l J(n) \Pi_c J(n-1) \cdots J(2) \Pi_c J(1) \Pi_r \\ &= \Pi_l \Pi_c J(n) \Pi_c J(n-1) \cdots J(2) \Pi_c J(1) \Pi_r \\ &= \pi\left(\tilde{P}(n)\right),\end{aligned} \quad (13)$$

where we define the new product $\tilde{P}(n) = K(n) \cdots K(2)K(1)$ of the projected matrices $K(i) = \Pi_c J(i)$.

Using the above description we obtain the sub-system LS for the homogeneous evolution. The projected Jacobian for the homogeneous evolution at time n is

$$J'(n) = \pi(J(n)) = \mu_n \pi(M) = \mu_n \cdot M' \quad (14)$$

where $M' = \pi(M)$ is the $N_s \times N_s$ constant matrix

$$M' = \begin{pmatrix} 1 - \varepsilon & \varepsilon/2 & 0 & \cdots & 0 \\ \varepsilon/2 & 1 - \varepsilon & \varepsilon/2 & \cdots & 0 \\ 0 & \varepsilon/2 & 1 - \varepsilon & \cdots & 0 \\ \vdots & \ddots & \ddots & \ddots & \vdots \\ 0 & \cdots & 0 & \varepsilon/2 & 1 - \varepsilon \end{pmatrix}$$

if $N_s < N$, and $M'_N = M$ if $N_s = N$. From now on we only use the notation M' when $N_s < N$. It is important to notice that by taking a sub-Jacobian matrix the periodicity of the boundary conditions is lost. The dynamics of the sub-system at the boundaries could be thought as being coupled to some external noise coming from the adjacent sites. Thus, in contrast to M , the matrix M' is not circulant, however its eigenvalues are well known to be [34]

$$\phi'_j(\varepsilon, N_s) = (1 - \varepsilon) + \varepsilon \cos\left(\frac{\pi j}{N_s + 1}\right). \quad (15)$$

(where $j = 1$ to N_s); and so the eigenvalues $\beta'_j(n)$ of $J'(n)$ are $\beta'_j(n) = \mu_n \phi'_j(\varepsilon, N_s)$. The sub-system LS is given by

$$\lambda'_j = \lambda_0 + \ln |\phi'_j(\varepsilon, N_s)|. \quad (16)$$

One can immediately infer from this that the Lyapunov exponents for the homogeneous evolution are interleaved for two consecutive sub-system sizes. More precisely, suppose that we take two sub-systems, one of size N_s and the other of size $N_s + 1$. It is then trivial to see that their respective Lyapunov exponents $\lambda'_i(N_s)$ and $\lambda'_i(N_s + 1)$ satisfy:

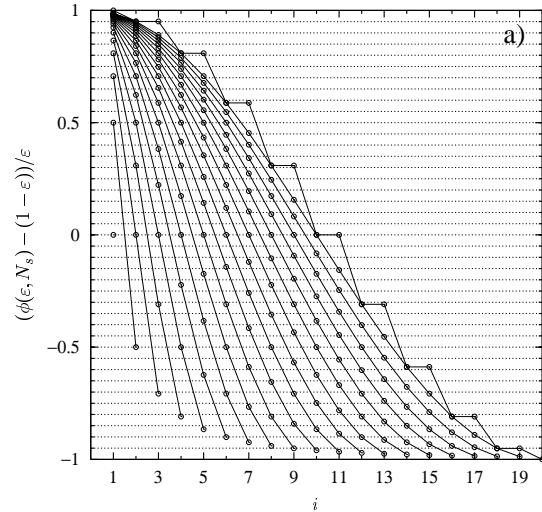
$$\lambda'_i(N_s + 1) \leq \lambda'_i(N_s) \leq \lambda'_{i+1}(N_s + 1) \quad \forall 1 \leq i \leq N_s, \quad (17)$$

see figure 1.a. Interleaving of the sub-system LS with respect to the whole LS $\lambda_i(N)$ also occurs:

$$\lambda_i(N) \leq \lambda'_i(N_s) \leq \lambda_{i+N-N_s}(N) \quad \forall 1 \leq i \leq N_s.$$

This interleaving of the eigenvalues is a consequence of Cauchy's interlace theorem [19] that gives bounds on the eigenvalues of a principal sub-matrix given the eigenvalues of the original matrix. It is important to notice that

the interleaving property of the Lyapunov exponents for the homogeneous case is a straightforward consequence of the decoupling of the time dependence of the Jacobian matrix leaving us with the constant matrices M and M' . In a typical non-homogeneous evolution the time dependence of the Jacobian cannot be factorized and an equivalent constant matrix for the Jacobian does not exist. Therefore, Cauchy's interlace theorem cannot be applied in this general case and there is no reason a priori for the interleaving property to hold for a generic extended dynamical system. It is true that, at any particular time, there is interleaving between the eigenvalues of the whole Jacobian and those of a sub-system. However, when computing the LS, one has to compute the product of the Jacobian matrices while for the sub-system LS one uses the product of the sub-Jacobian matrices and therefore the interleaving of the matrix product is no longer assured. The only way, a priori, for the interleaving to work would be to take the product of the whole Jacobians *first* and only then extract the sub-Jacobian. The problem with this procedure is that one has to rely again on re-orthonormalization procedures involving the original matrix size N , making the task impossible for large N . Nevertheless, as we shall see in the following section, the interleaving of the sub-system LS does hold to a great extent in the thermodynamic limit.



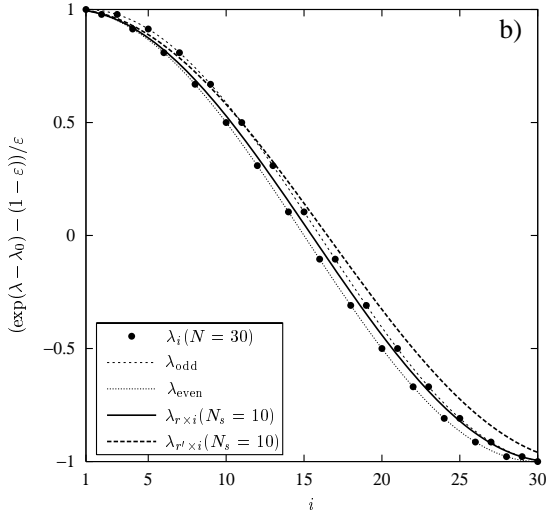


FIG. 1. Lyapunov spectrum for a homogeneous evolution in a diffusive CML: a) interleaving for sub-system sizes $N_s = 1, \dots, 20$ ($N = 20$); b) rescaled sub-system LS, the circles represent the whole LS ($N = 30$), the thin dashed lines represent the functions λ_{odd} and λ_{even} passing through the eigenvalues for even and odd indexes respectively, while the thick lines represent the rescaled LS with $N_s = 10$ using the conventional rescaling $r' = N/N_s$ (thick dashed line) and the new rescaling obtained in section II A $r = (N + 1)/(N_s + 1)$ (thick solid line).

Another important point to note from equations (15) and (16) is that the LS of the sub-systems all have the same shape. The best way to see this is to rescale the indices of the Lyapunov exponents so that they lie in the range $[0,1]$: so instead of plotting λ against j we plot it against $j/(N_s + 1)$. Equations (15) and (16) then show that the points always lie on the graph of the function

$$\lambda(z) = \lambda_0 + \ln [(1 - \varepsilon) + \varepsilon \cos(\pi z)], \quad (18)$$

irrespective of the value of N_s . This observation suggests another way of looking at the interleaving property. For a given N_s , the z values of the sub-system LS are equally spaced in the interval $[0,1]$; if we increase N_s by 1 the new z values interleave with the old. Since λ is a monotone function the fact that the z values interleave means that the $\lambda(z)$ values interleave also. It is worthwhile mentioning that we are considering the simple case $1 - 2\varepsilon > 0$ so the absolute value inside the logarithm in equation (16) can be omitted. For $1 - 2\varepsilon \leq 0$ the eigenvalues need further re-indexing in order to maintain their decreasing order and a similar construction as below is possible.

To compare the sub-system LS with that of the full system we should similarly rescale the indices for the latter, so now we plot the full system Lyapunov exponents against $j/(N + 1)$ instead of j . The points of this spectrum do not lie on the graph of $\lambda(z)$; however, equation (9) shows that they do lie on the graphs of the functions

$$\lambda_{\text{even}}(z) = \lambda(z(1 + 1/N))$$

(for exponents with even indices) and

$$\lambda_{\text{odd}}(z) = \lambda(z(1 + 1/N) - 1/N)$$

(for exponents with odd indices), where the function $\lambda(z)$ is given by equation (18). Since $z(1 + 1/N) - 1/N < z < z(1 + 1/N)$ ($0 < z < 1$) and $\lambda(z)$ is a decreasing function we see that $\lambda_{\text{even}}(z) < \lambda(z) < \lambda_{\text{odd}}(z)$. Thus λ_{even} and λ_{odd} are bounding curves for λ (see thin dashed lines in figure 1.b) and converge to it as $N \rightarrow \infty$; the differences between λ and the other curves are $\mathcal{O}(1/N)$.

The similarities between the shapes of the Lyapunov spectra of the sub-systems and of the whole system mean we can use the sub-system LS to estimate the whole LS: to do this we rescale the indices of the sub-system exponents, plotting λ_j against rj where r is a factor chosen so that the rescaled sub-system LS lies as close as possible to the plot of the full system LS. The above discussion shows that if we choose

$$r = \frac{N + 1}{N_s + 1} \quad (19)$$

then the rescaled sub-system LS differs from the full system LS by an amount of $\mathcal{O}(1/N)$.

The scaling given by (19) differs from that used conventionally, which is performed by scaling by

$$r' = \frac{N}{N_s}$$

see [4,12–14,35]. It is clear however that using r' will give results that differ from those using r by terms of $\mathcal{O}(1/N_s)$, and since this is larger than $\mathcal{O}(1/N)$ the errors in the exponents will also be $\mathcal{O}(1/N_s)$. This suggests that scaling (19) should give more accurate results than the conventional scaling; this is certainly true in the homogeneous case. As an example figure 1.b shows the original LS for a homogeneous CML with $N = 30$ (circles) along with the rescaled LS with $N_s = 10$ using the conventional rescaling r' (dashed line) and the new rescaling r obtained above (solid line). It is clear that the new rescaling gives a much better approximation to the original LS.

B. Interleaving and rescaling for coupled logistic maps

As mentioned in the previous section, the interleaving property for the homogeneous evolution relies on the fact that the Jacobian matrices can be factorized into a time dependent scalar and a *time independent* matrix (see equations (6) and (14)). For a non-homogeneous evolution the Jacobians cannot be factorized in such a way and thus *a priori* one does not expect interleaving to occur. Surprisingly enough the numerical evidence points towards interleaving of the sub-system LS for almost every Lyapunov exponent in the fully developed chaotic regime. In this section we shall present

such evidence for a logistic CML, and discuss why such behaviour might be expected to occur. More general systems will be considered in the following section.

We thus consider the diffusive CML (4) with the fully chaotic logistic map $f(x) = 4x(1-x)$ and compute its LS for several values of the coupling parameter ε . As with all numerical work in this paper we employ a fast HQR algorithm for the computation of Lyapunov exponents [8]. We then calculate the sub-system LS using principal sub-matrices J' of size $N_s = 1, \dots, 30$ of the Jacobian. In doing so one is not taking into account the dynamics of the neighbouring sites next to the boundary and their effects are considered as noise. Thus, the algorithm consists in computing the LS of the sub-Jacobian J' by truncating the actual Jacobian J at each time step and then applying the HQR algorithm. The results are shown in figure 2 where we plot the sub-system LS for increasing sub-system size ($N_s = 1, \dots, 30$) for 3 different values of the coupling parameter. In the figure, the filled circles represent the Lyapunov exponents that do not fulfil the interleaving condition. Strikingly, the LS corresponding to $\varepsilon = 0.05$ and $\varepsilon = 0.45$ (figures a and b) are very well interleaved, with the exception of a couple of points. On the other hand, for $\varepsilon = 0.95$ (figure c) the LS is not that well interleaved for the smallest Lyapunov exponents, although for the large ones the interleaving is as good as for the previous two figures. The reason for this failure for the smallest Lyapunov exponents is that in the limit $\varepsilon \rightarrow 1$ the lattice decouples into two independent sub-lattices: one for odd i and the other for even i . Thus, when successively increasing the sub-system size, one is including in turn contributions from the even and the odd sub-lattice. This is reflected in a variation in the smallest Lyapunov exponents every time we increase the sub-system size by one, hence the bi-periodic nature of the interleaving failure. In fact, by removing the sub-system LS for odd sizes one ends up with almost perfect interleaving. The exact reasons and conditions for the interleaving of the sub-system LS to happen are not yet understood, however we believe that they are connected with the convergence of the sub-system LS to the full system LS—a convergence which may be expected in the thermodynamic limit, see below.

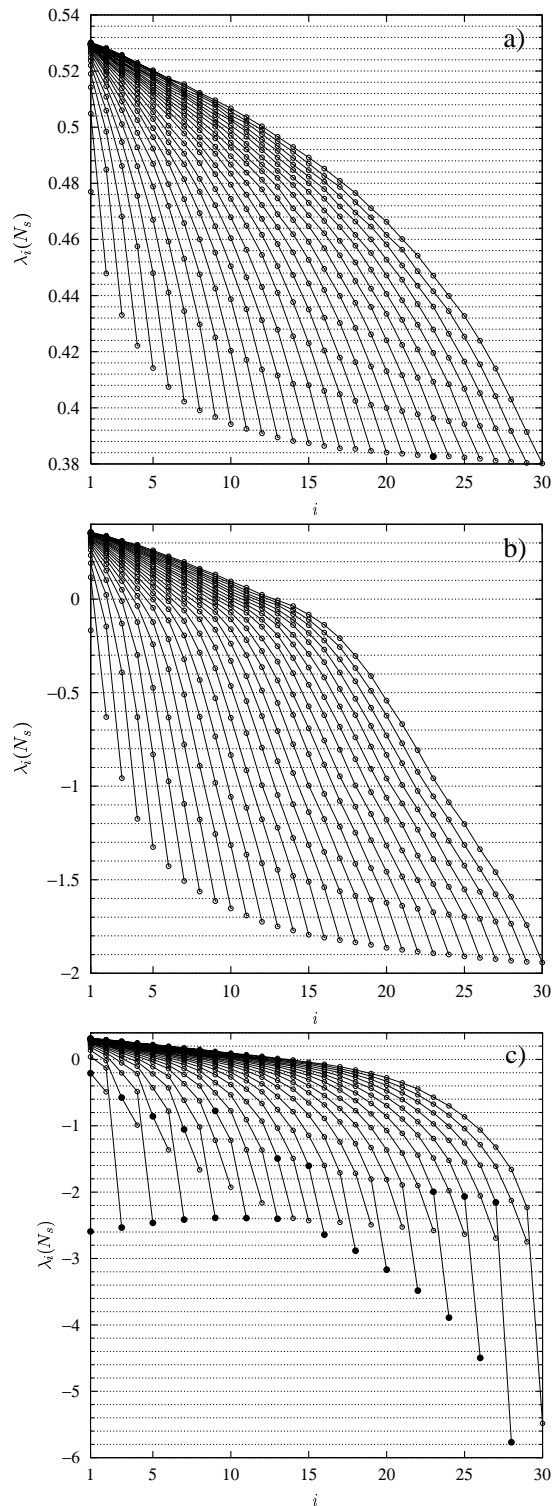


FIG. 2. Sub-system Lyapunov spectra for the fully chaotic coupled logistic lattice $N = 100$ for sub-system sizes 1 to 30 (left to right) for a) $\varepsilon = 0.05$, b) $\varepsilon = 0.45$ and c) $\varepsilon = 0.95$. The filled circles represent those Lyapunov exponents which fail to interleave.

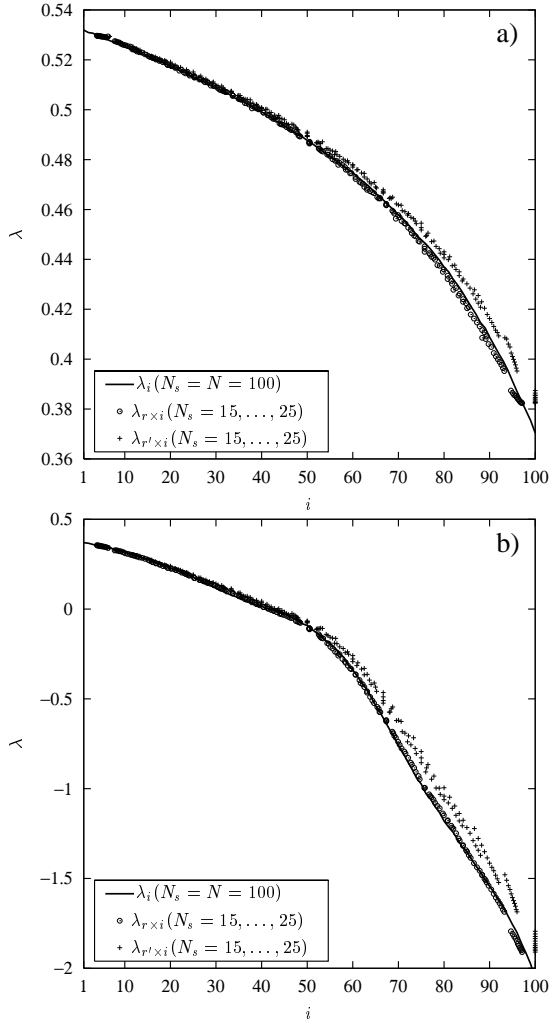


FIG. 3. Comparison of the whole Lyapunov spectrum (solid line) and the rescaled sub-system Lyapunov spectrum using the new rescaling r (circles) and the conventional rescaling r' (crosses) in the fully chaotic logistic lattice with $N = 100$ for several sub-system sizes ($N_s = 15, \dots, 25$). a) $\varepsilon = 0.05$ and b) $\varepsilon = 0.45$.

As mentioned in the introduction, it has been observed for some time that under appropriate rescaling the sub-system LS approximates the whole LS. The usual argument for this rescaling behaviour makes use of the thermodynamic limit. In the previous section, while studying the interleaving of sub-system LS for the homogeneous case, a new rescaling was suggested (see equation (19)). Let us test this for the case of the fully chaotic coupled logistic lattice. In figure 3 we compare, for $\varepsilon = 0.05$ and $\varepsilon = 0.45$, the rescaled sub-system LS using the new rescaling $r = (N + 1)/(N_s + 1)$ (19) (circles) and the conventional one $r' = N/N_s$ (crosses) to the whole LS (lines) for different sub-system sizes ($N_s = 15, \dots, 25$). As is clear from the figures, the new rescaling r gives a much better fit to the original LS than the conventional rescaling.

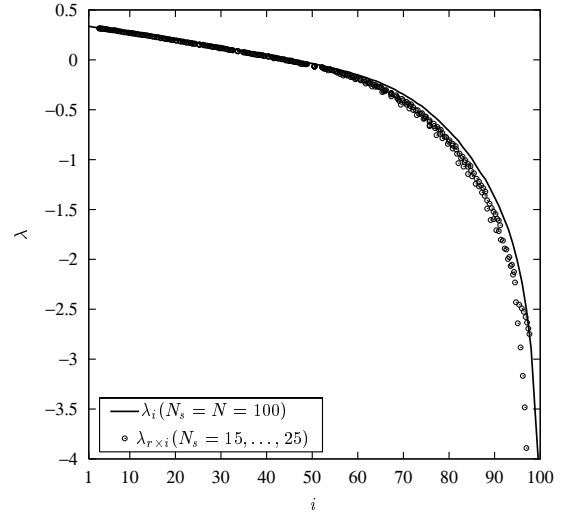


FIG. 4. Rescaled Lyapunov spectrum (circles) for the coupled logistic lattice with $\varepsilon = 0.95$ for sub-system sizes $N_s = 15, \dots, 30$. The solid line represents the whole Lyapunov spectrum $N_s = N = 100$.

Let us explore the idea of rescaling the sub-system LS in the thermodynamic limit a bit further. The correspondence between the rescaled LS and the whole LS in figure 3 is astonishingly good. The rescaled spectra lie almost perfectly on top of a decreasing curve, therefore, as with the homogeneous case discussed above, it is not surprising that they are interleaved. In general, if the rescaled Lyapunov spectra of the sub-systems converge sufficiently quickly to the whole system LS we expect to have good interleaving of the sub-system Lyapunov spectra. On the other hand, if the rescaled sub-system LS do not approximate the whole system LS well, it is not clear that interleaving will occur. To illustrate this we present the rescaled LS using the new rescaling r for $\varepsilon = 0.95$ in figure 4. In this case, the rescaled LS do not give such a good approximation to the whole LS (in particular for the smallest Lyapunov exponents) as seen in the other cases ($\varepsilon = 0.05$ and $\varepsilon = 0.45$). As explained above, this is due to the decoupling of the whole lattice into two sub-lattices when $\varepsilon \rightarrow 1$. Therefore it appears that the non-interleaving of the smallest Lyapunov exponents in figure 2.c is related to the lack of convergence of the sub-system LS. In general we suppose that failure to interleave is an indication that the sub-system LS have not converged. Clearly however, the presence of interleaving is not a sure indication that convergence has occurred; this is illustrated by the two-dimensional logistic lattice discussed below.

We believe that the key point in understanding the interleaving behaviour is that although in computing the sub-system LS one is using the product of projected matrices (13), one does not modify the original dynamics in any way. Recall that similar matrices share eigenvalues. Thus a feasible explanation for the occurrence of interleaving is to hypothesize that the product of the projected matrices $P'(n)$ is a projection of a $N \times N$ matrix $Q(\infty)$ which is similar to the limit as $n \rightarrow \infty$ of the original product $P(n)$ of the whole Jacobians. In

other words, we conjecture that there exists an invertible $N \times N$ matrix S such that

$$\mathcal{Q}(\infty) = \lim_{n \rightarrow \infty} S^{-1} P(n) S, \quad (20)$$

where the product of the projected matrices $P'(n)$ in the limit is obtained by projecting $\mathcal{Q}(\infty)$:

$$P'(\infty) = \pi(\mathcal{Q}(\infty)).$$

Informally, this is saying that in some sense in equation (13) the projection matrices commute on average with the Jacobians in the $n \rightarrow \infty$ limit. We believe that it might be possible to make this statement rigorous by an appropriate generalization of the multiplicative ergodic theorem.

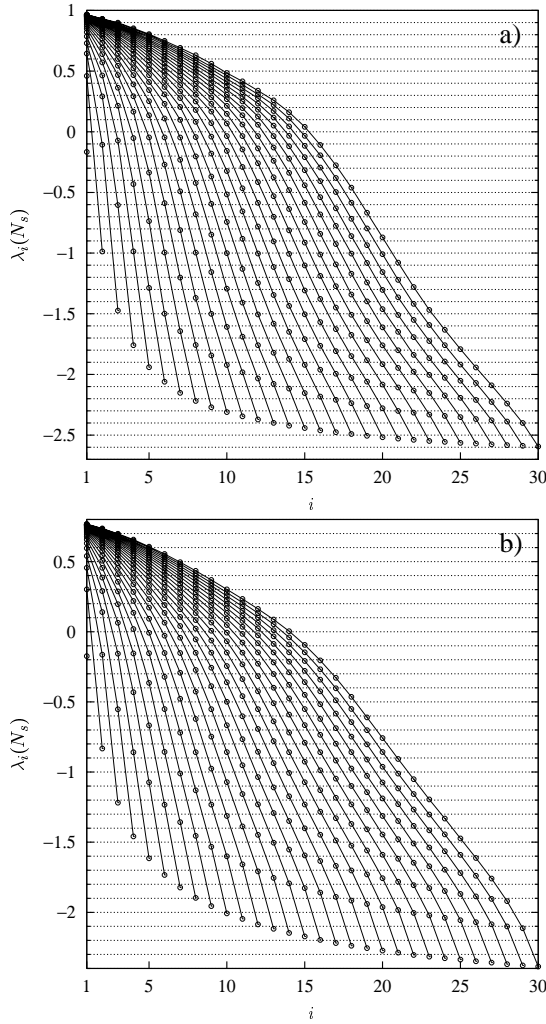


FIG. 5. Interleaving of the sub-system LS, $N_s = 1, \dots, 30$, for the fully chaotic logistic lattice with $\varepsilon = 0.45$ using the more general projection matrices (21) to extract the sub-system Jacobians: a) Π_1 and b) Π_2 .

One might then also ask what is so special about the projection Π_c . Is it possible for interleaving to occur for more general projections? The following two examples suggest that this is indeed the case. Consider the following projection matrices

$$\begin{aligned} \Pi_1 &= \left(\begin{array}{c|c} \Pi'_1 & Z \\ \hline Z^{\text{tr}} & 0 \end{array} \right) \\ \Pi_2 &= \left(\begin{array}{c|c} \Pi'_2 & Z \\ \hline Z^{\text{tr}} & 0 \end{array} \right) \end{aligned} \quad (21)$$

where Z is the $N_s \times (N - N_s)$ null matrix and the $N_s \times N_s$ matrices Π'_1 and Π'_2 are

$$\begin{aligned} \Pi'_1 &= \begin{pmatrix} 1 & 1 & 1 & \cdots & 1 \\ 0 & 1 & 1 & \cdots & 1 \\ 0 & 0 & 1 & \cdots & 1 \\ \vdots & \vdots & \vdots & \ddots & \vdots \\ 0 & 0 & 0 & \cdots & 1 \end{pmatrix} \\ \Pi'_2 &= \begin{pmatrix} 1 & \alpha_{12} & \alpha_{13} & \cdots & \alpha_{1N_s} \\ 0 & 1 & \alpha_{23} & \cdots & \alpha_{2N_s} \\ 0 & 0 & 1 & \cdots & \alpha_{3N_s} \\ \vdots & \vdots & \vdots & \ddots & \vdots \\ 0 & 0 & 0 & \cdots & 1 \end{pmatrix} \end{aligned}$$

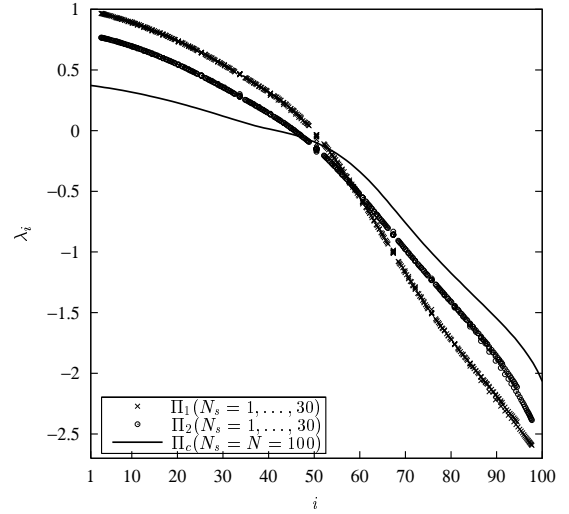


FIG. 6. Rescaled sub-system LS corresponding to figure 5 using the projection matrices Π_1 (crosses) and Π_2 (circles). The continuous line corresponds to the original LS computed with the whole Jacobian.

where the α_{ij} are random numbers chosen from the interval $[0, 1]$ with equal probability. Note that we are still using the term projection matrices for Π_1 and Π_2 which in a strict sense is not correct, since they do not satisfy $\Pi_j = \Pi_j^2$ ($j = 1, 2$). We use this terminology to stress the fact that they completely remove some of the entries of the original Jacobian. Thus, instead of taking the projection matrix Π_c let us take Π_1 and Π_2 . For the projection Π_2 we randomise its entries *every* time-step; similar results were obtained by randomising only at the beginning and keeping the same projection matrix thereafter. In figure 5 we depict the non-rescaled sub-system LS using both projection matrices for the

fully chaotic logistic lattice. The figure strongly suggests that in these cases interleaving still occurs. It thus appears that the choice of projection matrix is not a crucial ingredient for interleaving. Nonetheless it is important to say that we do not expect interleaving to hold if one uses a series of projection matrices such that when computing the LS one does not get convergence. In the above examples, Π_1 and Π_2 , we do have the required convergence. For the Π_2 case, the convergence of the LS of their product is a well known fact [36,37].

On the other hand, when we turn to rescaling we find that although for Π_1 and Π_2 we still get convergence of the rescaled sub-system LS to a definite limit, this limit is not the original LS for the full system (figure 6). The reason for this discrepancy is easy to understand since the new projections Π_1 and Π_2 combine the entries of the projected Jacobians and thus one expects the eigenvalues to change.

C. Estimation of quantities derived from the Lyapunov spectrum

As illustrated in the previous section, the LS can be well approximated by the rescaled sub-system LS in the thermodynamic limit. We now use the new rescaling in order to approximate the original LS by extrapolating from the sub-system LS. We estimate the largest Lyapunov exponent, Lyapunov dimension and KS entropy and we compare our method to the results obtained with the whole LS and with the conventional rescaling.

The first method to approximate quantities derived from the LS in the thermodynamic limit is by defining intensive quantities from the extensive ones by simply using the corresponding densities [38,16,12,35,5]. Let us define the densities of (1) and (2):

$$\begin{aligned} \rho_d(N_s) &= \frac{D_l}{N_s} \\ \rho_h(N_s) &= \frac{h}{N_s} \end{aligned} \quad (22)$$

corresponding to the Lyapunov dimension density and the KS entropy density respectively. In the thermodynamic limit these densities are intensive quantities (*i.e.* they do not depend on the sub-system size taken). One then estimates their extensive counterpart when $N_s \rightarrow N$ by multiplying the densities (22) by N . To estimate the largest Lyapunov exponent for the whole system we directly take the value of the largest Lyapunov exponent of the sub-system (the Lyapunov exponents are not extensive quantities). It is worth mentioning that in order to use these intensive densities to estimate extensive ones we are supposing the size N of the original system to be known.

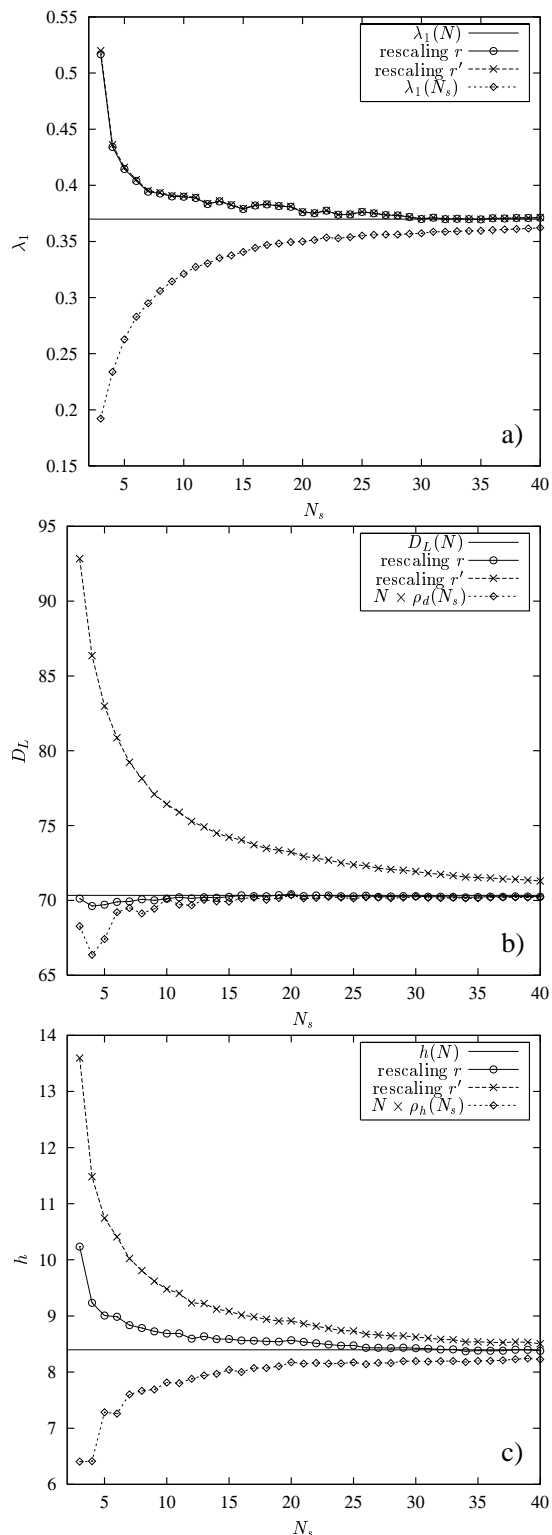


FIG. 7. Estimation of a) the largest Lyapunov exponent, b) the Lyapunov dimension and c) the KS entropy as a function of the sub-system size N_s in the coupled logistic lattice with $N = 100$ and $\varepsilon = 0.45$. The estimates obtained by using a) the largest Lyapunov exponent of the sub-system and b-c) the associated densities from the sub-system are presented with diamonds, and the estimate obtained from the piece-wise linear fit to the rescaled LS is presented with crosses for the conventional rescaling and circles for the proposed new one. The values obtained with the whole LS are represented by the horizontal line.

The second method, which we believe is more accurate, consists of taking the sub-system LS, rescaling it, extrapolating a curve through it to obtain an approximation to the whole LS and only then computing the desired quantities. There are several ways to extrapolate the whole LS from the sub-system LS; here we have chosen a piece-wise linear approximation for simplicity. One could use more accurate methods such as cubic splines but the aim here is to compare both kinds of rescaling and thus a piece-wise linear fit is the most straightforward approach. Therefore, take the rescaled LS $\lambda_i(N_s)$, obtained with either rescaling for a sub-system of size N_s , and consider the polygon \mathcal{P} through all the points $(i, \lambda_i(N_s))$. To estimate a Lyapunov exponent of the whole LS lying between $\lambda_1(N_s)$ and $\lambda_{N_s}(N_s)$ one simply uses the fit given by the polygon \mathcal{P} . For Lyapunov exponents lying to the left (right) of the polygon use linear extrapolation from the first (last) two points of the rescaled LS. Here again one could use more sophisticated extrapolation methods but for simplicity we restrict ourselves to the linear one. Once the whole LS is estimated using the above method, or a more complicated one, quantities such as the largest Lyapunov exponent $\lambda_1(N)$, the Lyapunov dimension D_L and the KS entropy h are easily extracted.

In figure 7 we compare the estimates of a) the largest Lyapunov exponent $\lambda_1(N)$, b) the Lyapunov dimension D_L and c) the KS entropy h obtained from the intensive densities (diamonds) and the piece-wise linear fitting for both rescalings (conventional rescaling with crosses and the proposed new one with circles) as the sub-system size increases for the coupled logistic lattice. The actual values of these quantities calculated with the whole LS correspond to the horizontal lines. For the largest Lyapunov exponent, figure 7.a, we notice that the estimates are almost identical for both rescalings (crosses and circles). This is due to the fact that both rescalings tend to coincide for small i (see figure 1.b). The estimate of the largest Lyapunov exponent by just taking the largest Lyapunov exponent of the sub-system (diamonds) shows a slower convergence than the linear fit methods. For the Lyapunov dimension, figure 7.b, the method with the slowest convergence corresponds to the conventional rescaling (crosses), while the approximations derived from densities (diamonds) and from a linear fit with the new rescaling (circles) are quite good (note that the new rescaling method does better than the approach using densities). Finally, for the KS entropy, figure 7.c, the estimates using the density (diamonds) and the conventional rescaling (crosses) have similar convergence rates while the new rescaling method (circles) does considerably better. The evidence given by this set of plots tends to indicate that the new rescaling method gives better convergence to the quantities derived from the sub-system LS.

III. MORE GENERAL EXTENDED DYNAMICAL SYSTEMS

So far we have only considered interleaving and rescaling in systems in one spatial dimension with nearest neighbour coupling, corresponding to tridiagonal Jacobians. In this section we turn to more general kinds of extended dynamical systems by allowing a larger coupling range (*e.g.* chaotic neural networks) and by taking a different topology for the lattice (*e.g.* lattice with two spatial dimensions). The results presented in this section suggest that the interleaving and rescaling properties observed for the simpler one-dimensional CML persist for more general extended dynamical systems.

A. Chaotic neural networks

We now consider a chaotic neural network [12] of the form

$$x_i^{n+1} = \tanh \left(g \sum_{l=i-k}^{i+k} C_{il} x_l^n \right), \quad (23)$$

where g is a real number called the gain parameter, k represents the connectivity (essentially playing the same role as the range of the coupling in a CML) and the weight matrix C_{ij} has entries chosen randomly from $[-1, 1]$ with a uniform probability distribution for $(i - j) \pmod{N} \leq k$ and $C_{ij} = 0$ otherwise.

Both the CNN and CML dynamics work in two stages—nonlinearity and coupling—but their order is inverted. The CML dynamics applies the nonlinear mapping f first and then the coupling, while the CNN first applies the coupling via a linear weighted combination of neighbouring sites, and then a nonlinear map (the sigmoid). This inversion is reflected in the Jacobian matrix of the transformation: while each entry of the CML Jacobian (6) depends on a single site, each entry of the CNN Jacobian depends on a neighbourhood of sites:

$$J_{ij}(n) = \frac{g C_{ij}}{\cosh^2 \left[\sum_{l=i-k}^{i+k} C_{il} x_l^n \right]}. \quad (24)$$

The CNN Jacobian (24) inherits the zeros of the coupling matrix C_{ij} , *i.e.* $J_{ij}(n) = 0$ if $(i - j) \pmod{N} > k$. Another difference between the CNN that we will consider and the diffusive CML discussed before is that the CNN involves coupling with a larger neighbourhood than just the left and right nearest neighbours.

Let us now analyze the interleaving and rescaling for a CNN with a large k . In figure 8 we show the interleaving and rescaling with $k = 10$ and $g = 2$. As we can see, the interleaving is quite good with the exception of a few small Lyapunov exponents. In figure 8.b we plot the rescaled sub-system LS for several sub-system sizes

using both rescalings (circles: new rescaling and crosses: conventional rescaling) along with the whole LS (solid line). Clearly the new rescaling gives a better estimate of the whole LS. Similar results were obtained for other values of the parameters k and g .

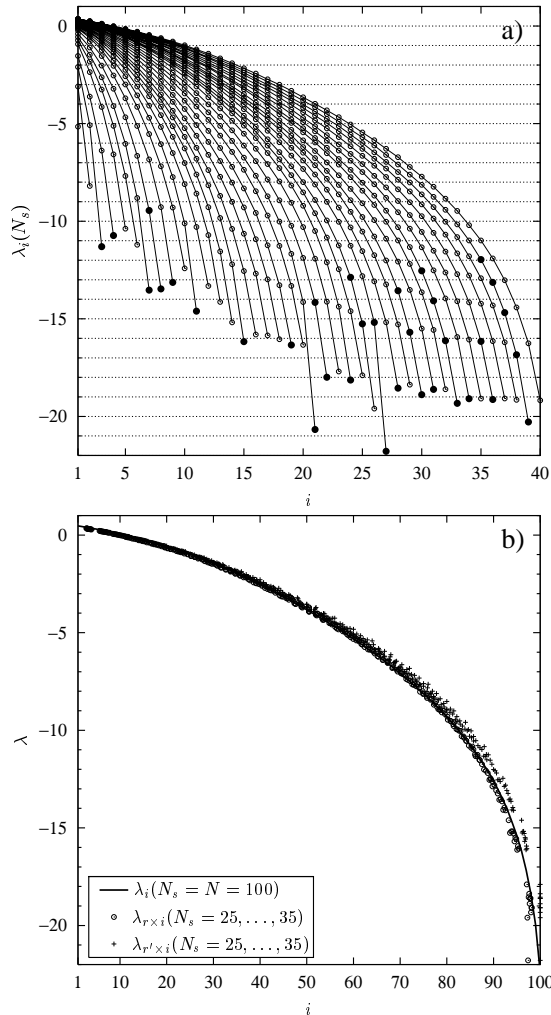


FIG. 8. a) Interleaving of the sub-system LS in the chaotic neural network (23) with $k = 10$ and $g = 2$. b) Comparison between the conventional rescaling of the sub-system Lyapunov spectrum (crosses) and the new rescaling obtained in section IIA (circles), the whole LS is depicted by the solid line.

B. Two-dimensional logistic lattice

The interleaving and rescaling properties of the sub-system LS were obtained in section IIA for a one-dimensional array of coupled maps. Here we put to the test the interleaving and rescaling for a two-dimensional CML. Let us take a two-dimensional square lattice of size $L \times L$. The local dynamics x_{ij}^n at each node (i, j) and any time n is governed by the fully chaotic logistic map

$$f_{ij}(x) = f(x) = 4x(1-x).$$

As in the one-dimensional CML the local dynamics is applied first

$$y_{ij}^n(x) = f(x_{ij}^n),$$

and then the coupling dynamics

$$x_{ij}^{n+1} = (1-\varepsilon)y_{ij}^n + \varepsilon \overline{y}_{\mathcal{N}_{ij}}^n,$$

where $\overline{y}_{\mathcal{N}_{ij}}^n$ is the average of the y_{ij}^n in the neighbourhood \mathcal{N}_{ij} of site (i, j) . The neighbourhood \mathcal{N}_{ij} is taken to be the eight adjacent sites to (i, j) with periodic boundary conditions.

The Jacobian $J(n)$ at time n for this two-dimensional lattice is defined through its elements:

$$J_{kl}(n) = \frac{\partial x_{\sigma_k}^{n+1}}{\partial x_{\sigma_l}^n},$$

where the indices σ_k and σ_l refer to the position in the actual lattice of the chosen k th and l th state variables of the system. If one just wants to compute eigenvalues of the whole Jacobian, the order in which the state variables are taken is not relevant. However we are interested in extracting sub-Jacobian matrices from the whole system and thus the ordering choice of the state variables does matter. There are $L^2!$ different ways to choose the ordering, but the simplest way consists of taking the site $(1,1)$ as the first state variable and then proceeding horizontally to the right until the end of the lattice is reached and then proceeding to the bottom of the lattice by rows:

1	2	3	...	$L-1$	L
$L+1$	$L+2$	$L+3$...	$2L-1$	$2L$
$2L+1$	$2L+2$	$2L+3$...	$3L-1$	$3L$
\vdots	\vdots	\vdots		\vdots	\vdots

that is $\sigma_k = (k - \lfloor k/L \rfloor, \lfloor k/L \rfloor)$ where $\lfloor z \rfloor$ denotes the largest integer smaller than or equal to z . From now on this kind of ordering will be called *horizontal wraparound*. There is obviously a vertical counterpart where the order is taken by columns. The problem with this type of ordering is that it does not build up the Jacobian in a natural way. The propagation of a perturbation typically grows equally in both of the two spatial dimensions (in particular for our choice of coupling since all the neighbours contribute with the same weight $\varepsilon/8$). In contrast, with horizontal or vertical wraparound one has to wait until a complete wrap is taken to fall again near the perturbed area. A more natural approach might thus be to attempt to mimic the spatial growth of perturbations by taking an ordering that fills up a two-dimensional area from the centre outwards. For that purpose, we use the following ordering technique:

1	2	5	10	...
4	3	6	11	...
9	8	7	12	...
16	15	14	13	...
⋮	⋮	⋮	⋮	⋮

We call this *square wraparound*.

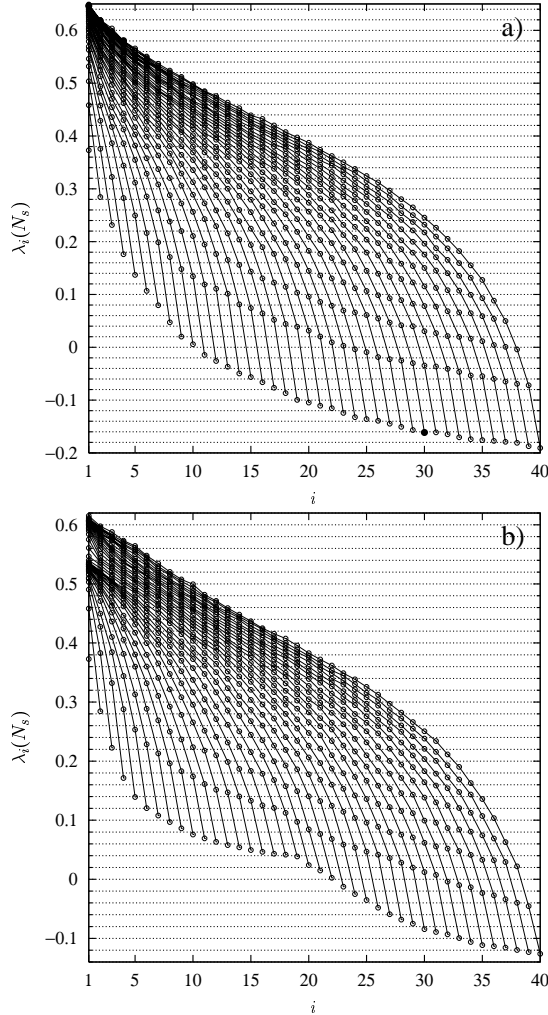


FIG. 9. Sub-system Lyapunov spectra for the two-dimensional 20×20 coupled logistic lattice for sub-system sizes 1 to 40 (left to right) for $\varepsilon = 0.45$ and for the two wraparound methods for building up the Jacobian: a) square wraparound and b) horizontal wraparound. The filled circles represent the Lyapunov exponents where interleaving fails.

In figure 9 we show the non-rescaled sub-system LS for the two wraparound methods, a) square and b) horizontal, and we plot with solid circles the Lyapunov exponents that fail to interleave. Observe that interleaving failure occurs for only a very few Lyapunov exponents. After a careful examination of these Lyapunov exponents one notices that they are very close to interleaving, suggesting that the failure is due to numerical error

in the computation of the exponents (and in particular poor convergence). Therefore, we shall consider a Lyapunov exponent to be interleaved if it falls in the interval defined by the inequality (17) with an error δ :

$$\lambda_i(N_s + 1) - \delta\Lambda \leq \lambda_i(N_s) \leq \lambda_{i+1}(N_s + 1) + \delta\Lambda, \quad (25)$$

where $\Lambda = \lambda_{i+1}(N_s + 1) - \lambda_i(N_s + 1)$. From now on we redefine δ such that the errors are given in percentages. Using such a definition, if one allows a small error of 2.5% — $\delta = 0.025$ in (25)— for the Lyapunov exponents in figure 9, one obtains perfect interleaving for the whole spectrum.

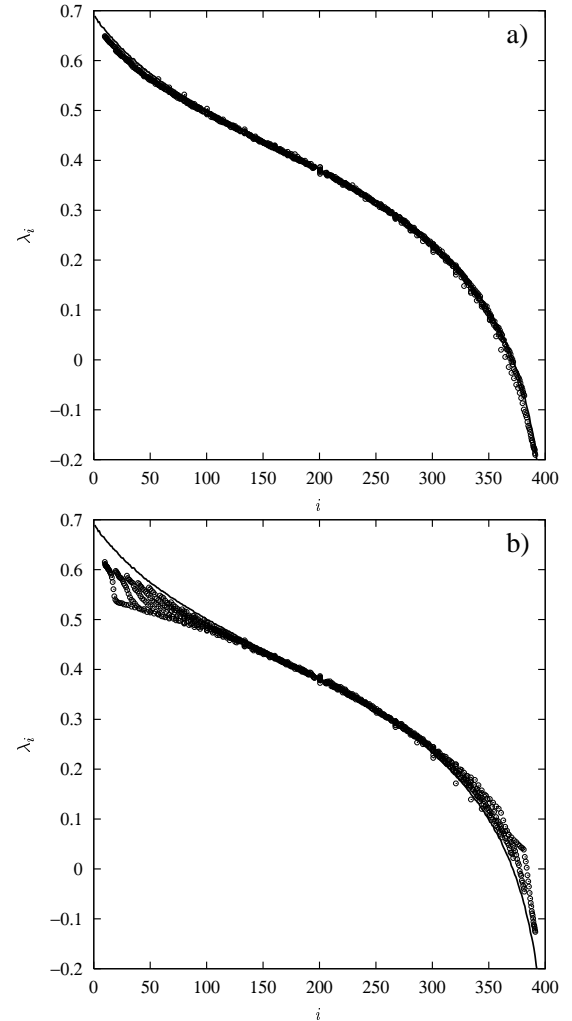


FIG. 10. Rescaled sub-system LS for the two-dimensional coupled logistic lattice (same parameters as in figure 9) using a) square and b) horizontal wraparound methods.

The interleaving seen in figure 9 suggests that the ordering choice for the Jacobian entries does not play an important role in this phenomenon. However, as can be seen in figure 10, where we plot the rescaled LS for both wraparound methods along with the whole LS, the choice of ordering method is crucial in obtaining good rescaling behaviour. Square wraparound (figure 10.a) yields immediate convergence towards the whole LS: even for a very small sub-system size the rescaled LS

is almost exactly superimposed on top of the whole LS. On the other hand, horizontal wraparound (figure 10.b) gives a rescaled sub-system LS that seems to converge to a different curve for sub-system sizes $N_s = 1, \dots, 20$ (aligned points in the lower part of the curve for the first Lyapunov exponents). For sub-system sizes larger than 20 the rescaled LS starts a new convergence towards something closer to the whole LS. The explanation for this phenomenon is quite simple. The Jacobian for the horizontal wraparound consists of a main diagonal of non-zero elements coming from the neighbours in the same row of the square lattice, however, the neighbours in the row above and below give rise to two sub-diagonals of non-zero elements. The sub-diagonals start when a whole wraparound has been completed, that is when $N_s = L$ where L is the side length of the square lattice. Thus for sub-system sizes $N_s < L$ the sub-Jacobian only extracts the main diagonal elements and does not capture the two sub-diagonals with vital information about the neighbouring sites in the rows above and below. When $N_s \geq L$ the sub-Jacobian starts capturing these forgotten neighbours and the rescaled sub-system LS now begins to converge to the desired LS. For the example in figure 10.b this behaviour starts at $N_s = L = 20$. This effect of horizontal wraparound is reflected when one tries to extract information from the sub-system LS. As an example, we depict in figure 11 an estimate of the largest Lyapunov exponent by extrapolating the whole LS from its rescaled version as the sub-system size increases. The results are depicted with circles for square wraparound and with crosses for horizontal wraparound. The vertical solid line corresponds to the largest Lyapunov exponent from the whole LS. The estimate using horizontal wraparound seems to converge to a much smaller value than the desired one for sub-system sizes $N_s < L = 20$. When the sub-system size is increased further, horizontal wraparound performs better but still lacks the desired convergence. On the other hand, the square wraparound converges rapidly in a smooth way: this is because it was designed to build up the Jacobian entries in a more natural way. Therefore, although the interleaving for both wraparound methods is very good it is considerably more reliable to use the square wraparound for rescaling purposes of the sub-system LS.

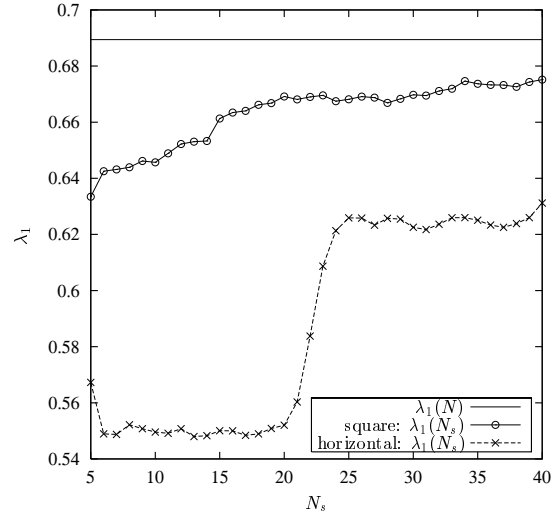


FIG. 11. Estimation of the largest Lyapunov exponent as a function of the sub-system size N_s in a two-dimensional logistic lattice of size 20×20 and with $\varepsilon = 0.45$ using a linear fit for the rescaled sub-system LS. The circles correspond to building up the Jacobian by square wraparound whilst the crosses correspond to horizontal wraparound. The value of the largest Lyapunov exponent for the whole lattice is represented by the horizontal solid line.

C. Host-parasitoid system

We now consider a more general type of two dimensional lattice, namely the Host-Parasitoid lattice model [39–41]. For this system the local dynamics is no longer one-dimensional but two-dimensional: hosts and parasitoids. The model evolves again in two phases. First there is at each site (i, j) a local dynamics given by

$$\begin{aligned} \mathcal{H}_{ij}^n &= bH_{ij}^n e^{-aP_{ij}^n} \\ \mathcal{P}_{ij}^n &= cH_{ij}^n \left(1 - e^{-aP_{ij}^n}\right) \end{aligned} \quad (26)$$

where H^n and P^n are respectively the population size of hosts and parasitoids at time n , a is the per capita parasitoid attack rate, b is the host reproductive rate and c is the conversion efficiency of parasitised hosts into female parasitoids in the next generation. The second phase involves dispersal into a neighbourhood \mathcal{N}_{ij} of site (i, j) , *i.e.* a fraction μ_h of hosts and μ_p of parasitoids disperse equally into the eight neighbouring sites:

$$\begin{aligned} H_{ij}^{n+1} &= (1 - \mu_h) \mathcal{H}_{ij}^n + \mu_h \overline{\mathcal{H}}_{\mathcal{N}_{ij}}^n \\ P_{ij}^{n+1} &= (1 - \mu_p) \mathcal{H}_{ij}^n + \mu_p \overline{\mathcal{P}}_{\mathcal{N}_{ij}}^n \end{aligned} \quad (27)$$

where $\overline{\mathcal{H}}_{\mathcal{N}_{ij}}^n$ and $\overline{\mathcal{P}}_{\mathcal{N}_{ij}}^n$ are, respectively, the average of the hosts and the parasitoids (after local dynamics (26)) in the neighbourhood \mathcal{N}_{ij} of site (i, j) . We take a square lattice $(i, j) \in [1, L]^2$ and periodic boundary conditions. The total size of the system is then $N = 2L^2$. Let us build up the whole Jacobian with host-parasite blocks of size 2×2 :

$$J = \begin{pmatrix} \mathcal{J}_{\sigma_1}^{\sigma_1} & \mathcal{J}_{\sigma_2}^{\sigma_1} & \cdots & \mathcal{J}_{\sigma_{L^2}}^{\sigma_1} \\ \mathcal{J}_{\sigma_1}^{\sigma_2} & \mathcal{J}_{\sigma_2}^{\sigma_2} & \cdots & \mathcal{J}_{\sigma_{L^2}}^{\sigma_2} \\ \vdots & \vdots & \ddots & \vdots \\ \mathcal{J}_{\sigma_1}^{\sigma_{L^2}} & \mathcal{J}_{\sigma_2}^{\sigma_{L^2}} & \cdots & \mathcal{J}_{\sigma_{L^2}}^{\sigma_{L^2}} \end{pmatrix},$$

where the host-parasite blocks $\mathcal{J}_{\sigma_j}^{\sigma_i}$ are given by

$$\mathcal{J}_{\sigma_j}^{\sigma_i} = \begin{pmatrix} \frac{\partial H_{\sigma_i}^{n+1}}{\partial H_{\sigma_j}^n} & \frac{\partial H_{\sigma_i}^{n+1}}{\partial P_{\sigma_j}^n} \\ \frac{\partial P_{\sigma_i}^{n+1}}{\partial H_{\sigma_j}^n} & \frac{\partial P_{\sigma_i}^{n+1}}{\partial P_{\sigma_j}^n} \end{pmatrix}.$$

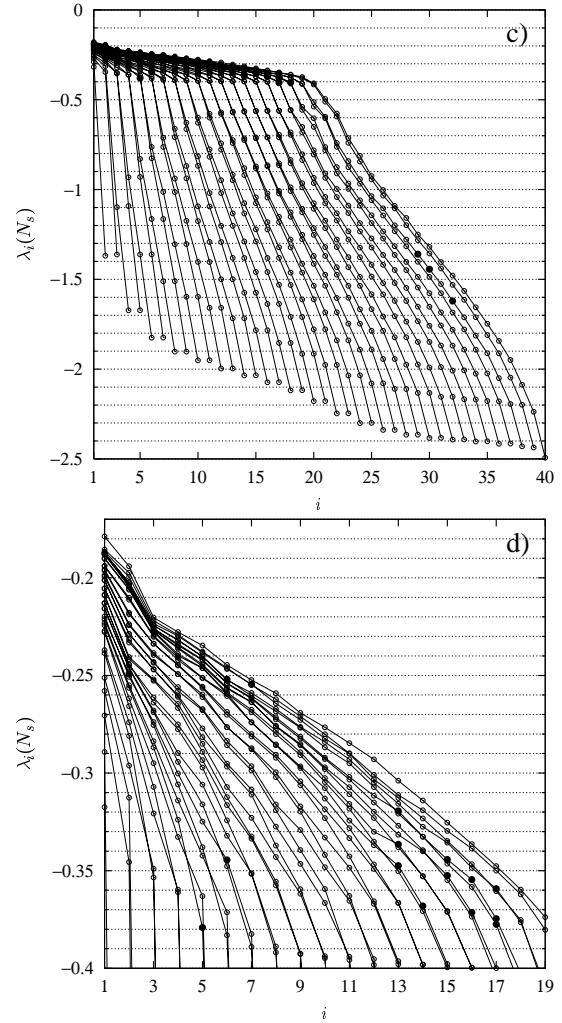
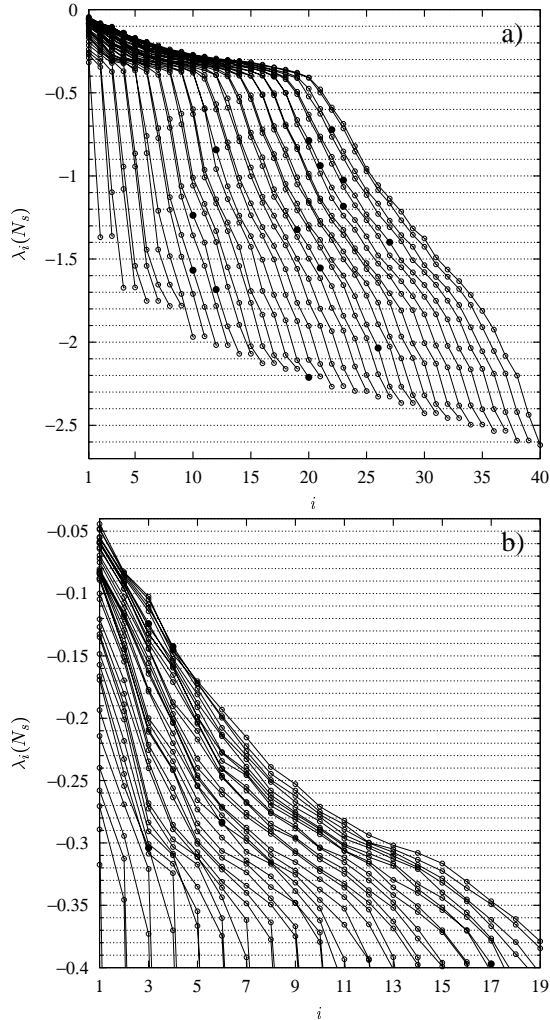


FIG. 12. Interleaving of the sub-system LS for the host-parasite system in a two-dimensional lattice of size 20×20 . The Jacobian was built using a)–b) square wraparound and c)–d) horizontal wraparound. Figures b) and d) correspond, respectively, to amplifications of figures a) and c) for the top half of the spectrum.

The indices σ_1, \dots, L^2 refer to the actual position in the two-dimensional lattice of a particular local population. As for the two-dimensional CML the ordering choice of the Jacobian entries plays an important role for the rescaling.

Given a reasonable lattice size ($L > 15$) and depending on the dispersal parameters μ_h and μ_p the evolution of model (27) is spatio-temporally chaotic [42]. Here we choose $L = 20$, $a = 1$, $b = 2$, $c = 1$, $\mu_h = 0.2$ and $\mu_p = 0.6$. The full system is thus $N = 2L^2 = 800$ dimensional. We start the system with random initial conditions and discard a transient of 10^5 iterations before computing the sub-system LS. In figure 12 we depict the interleaving of the sub-system LS for sub-system sizes $N_s = 1, \dots, 40$ where we allow a 5% error in the interleaving — $\delta = 0.05$ in (25). Figures 12.a and 12.b correspond to square wraparound whilst figures 12.c and 12.d correspond to horizontal wraparound. As the figure shows, interleaving is quite good even for the upper re-

gion (see amplifications in figures 12.b and 12.d) where the density of Lyapunov exponents is very high and the intervals for interleaving are small and thus the margin for error in the inequality (25) is reduced. Square wraparound does better for large Lyapunov exponents (figure 12.b) whilst horizontal wraparound does better for small ones. However, overall both methods have approximately similar performance.

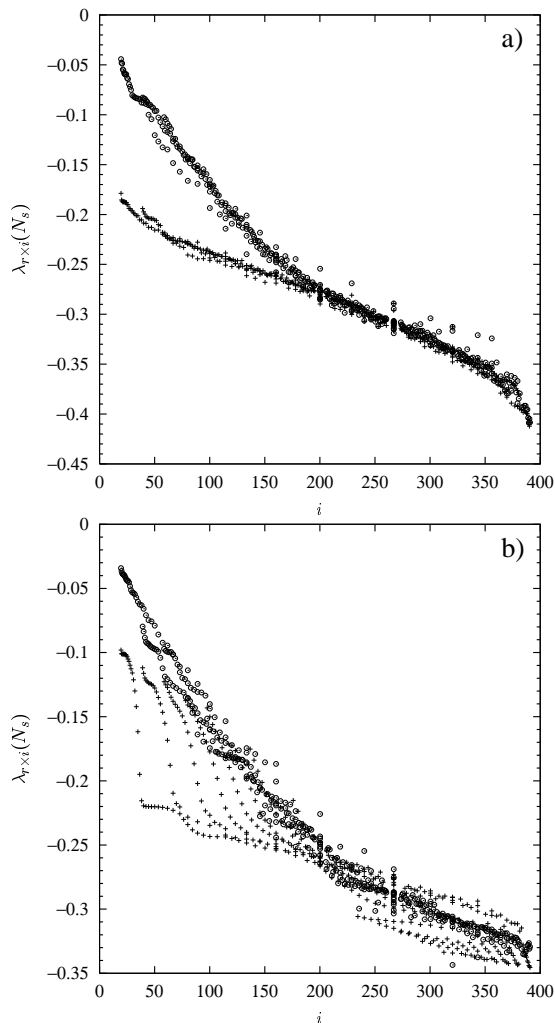


FIG. 13. First half of the rescaled Lyapunov spectrum for a host-parasitoid system in a two-dimensional lattice for sub-system sizes $N_s = 1, \dots, 40$. a) Using both the host and parasite variables and b) using only the hosts when building up the Jacobian. The circles (crosses) correspond to the square (horizontal) wraparound.

While the choice of wraparound method is not crucial for interleaving, figure 13.a shows that it leads to significant differences in rescaling behaviour. Note that the LS for the whole system $N_s = N = 800$ is not depicted since it would take an enormous amount of time to compute. In figure 13.a we depict the rescaled LS for sub-system sizes $N_s = 1, \dots, 40$ for both wraparound methods (square wraparound with circles and horizontal wraparound with crosses). As for the two-dimensional lattice of coupled logistic maps, horizontal wraparound converges to a different curve than

does square wraparound. The reason is again that for the horizontal wraparound one has to wait until a complete wrap is finished until falling again into the neighbouring region. In this case, a horizontal wrap of the Jacobian is achieved when $N_s = 2L = 40$. Moreover, for $N_s = 2L = 40$ one is only including partial derivatives of hosts with respect to hosts and parasitoids. In order to include dependences of parasitoids with respect to hosts and parasitoids one should take a further wrap of the Jacobian, *i.e.* $N_s = 4L = 80$.

Therefore, the horizontal wraparound technique for sub-system sizes $N_s \leq 40$ does not pick up the dynamics of the neighbours situated in adjacent rows. This problem for horizontal wraparound becomes worse as the dimension of the local dynamics is increased. A partial solution to this problem is to build up the Jacobian by using just one of the local variables of the system. Particularly in the host-parasite system where the parasitoid dynamics is slaved to the host dynamics, one should be able to reproduce the LS from only the host variables. We then build up the Jacobian by taking only host variables using both wraparound methods. The results are shown in figure 13.b where again the circles correspond to square wraparound and the crosses to horizontal wraparound. We only plot the first half of the spectrum, the second half of the spectrum differs considerably for both methods (host-parasites variables and only host variables) since the small Lyapunov exponents are more sensitive to the loss of information contained in the parasite variables. On the other hand, the first half of the spectrum is quite similar independently of the choice of host-parasite or only host variables. As we can see in figure 13.b, horizontal wraparound seems to converge to a different curve than square wraparound for sub-system sizes $N_s < 20$ (see aligned crosses in the lower part of the spectrum). Since we are only taking the host population (20×20), when $N_s > 20$ the horizontal wraparound has finished a complete wrap and it starts to pick up the neighbours in adjacent rows and thus the rescaled spectrum begins to converge closer to the square wraparound.

IV. CONCLUSIONS

When studying high dimensional extended dynamical systems in a spatio-temporal chaotic regime it is possible to rescale the sub-system Lyapunov spectrum to obtain the original Lyapunov spectrum. In this thermodynamic limit, a sub-system of comparatively small size N_s contains a sufficient amount of information to reconstruct the Lyapunov spectrum of the whole system. Usually, when coupling different sub-systems in a lattice one chooses a coupling with a finite neighbourhood (localized coupling) or at least with decreasing effect for further away neighbours. In the context of discrete spatio-temporal systems, this restriction on the choice of coupling causes the Jacobian of the dynamics to be a banded (or quasi-banded) matrix. In the limit of only

nearest neighbours interaction in a one-dimensional lattice, the Jacobian is a tridiagonal matrix. If one considers the homogeneous evolution under this dynamical system, the Lyapunov spectrum of sub-Jacobian matrices will inherit the rescaling and interleaving properties described in section II A. The evidence presented in this paper shows that the new rescaling method of the sub-system Lyapunov spectrum gives a much better fit than the conventional rescaling N/N_s for one-dimensional lattices.

We have also observed interleaving of the Lyapunov spectra for consecutive sub-system sizes. We showed that for two-dimensional lattices the rescaling and interleaving are still valid. However, the choice of variables used to build up the sub-Jacobian matrices appears to be crucial to achieve good rescaling properties. In particular one has to choose an ordering method of the system variables that mimics the propagation of information in the particular lattice topology of the system. In two dimensions we showed that choosing the system variables in ‘concentric’ sub-squares gave a much better rescaled Lyapunov spectrum than by choosing them in a row or column-wise fashion. Generalizing this idea to higher-dimensional lattices one should take the system variables by filling up ‘concentric’ hyper-cubes.

Another point to take into account when choosing the system variables in high-dimensional lattices is the anisotropy of the coupling. The two-dimensional systems studied here have an equal relative contribution from all the neighbouring directions (isotropic coupling). It is possible to choose the coupling in order to give more weight to one of the directions (vertical or horizontal) and thus the propagation of information to be faster in that direction. Therefore, instead of building the system variables by ‘concentric’ squares it should be more natural to take rectangles, the ratio of the rectangle sides being related to the ratio of velocity propagation of disturbances in both directions.

For a continuous spatio-temporal system a similar reconstruction may be used by sampling in a grid of a sub-system at regular time intervals and by reconstructing the Jacobian from time series in the usual manner. The same procedure can be applied for a discrete spatio-temporal system where the dynamics is not explicitly given and the only available dynamic information comes from time series taken at several spatial locations. We expect that rescaling and interleaving should still be observed in these cases. This aspect is currently under investigation and will be reported elsewhere [43].

ACKNOWLEDGMENTS

This work was carried out under an EPSRC grant number GR/L42513. JS would also like to thank the Leverhume Trust for financial support under a Royal Society Leverhume Trust Senior Research Fellowship.

REFERENCES

- [1] J.L. Kaplan and J.A. Yorke. Chaotic behaviour of multidimensional difference equations. *Lecture Notes in Mathematics*, Springer, New York, **730** (1979) 204–227.
- [2] H.G. Schuster. *Deterministic chaos*. VCH Verlagsgesellschaft, Weinheim, second edition, 1988.
- [3] J.-P. Eckmann and D. Ruelle. Ergodic theory of chaos and strange attractors. *Rev. Modern Phys.* **57**, 3 (1985) 617–656.
- [4] P. Grassberger. Information content and predictability of lumped and distributed dynamical systems. *Phys. Scr.* **40** (1989) 346–353.
- [5] G.P. Puccioni A. Torcini, A. Politi and G.D’Alessandro. Fractal dimension of spatially extended systems. *Physica D* **53** (1991) 85–101.
- [6] M. Bauer, H. Heng and W. Martienssen. Characterization of spatiotemporal chaos from time series. *Phys. Rev. Lett.* **71**, 4 (1993) 521–524.
- [7] K. Geist, U. Parlitz and W. Lauterborn. Comparison of different methods for computing Lyapunov exponents. *Prog. Theor. Phys.* **83**, 5 (1990) 875–893.
- [8] H.F. von Bremen, F.E. Udvardia and W. Proskurowski. An efficient QR based method for the computation of Lyapunov exponents. *Physica D* **101** (1997) 1–16.
- [9] D. Ruelle. Large volume limit distribution of characteristic exponents in turbulence. *Commun. Math. Phys.* **87** (1982) 287–302.
- [10] Ya.G. Sinai. A remark concerning the thermodynamic limit of the Lyapunov spectrum. *Int. J. Bifurcation and Chaos* **6**, 6 (1996) 1137–1142.
- [11] Ya.G. Sinai and N.I. Chernov. Entropy of a gas of hard spheres with respect to the group of space-time shifts. *Proc. of Petrovski Seminar* **8** (1982) 218–238.
- [12] M. Bauer and W. Martienssen. Lyapunov exponents and dimensions of chaotic neural networks. *J. Phys. A* **24** (1991) 4557–4566.
- [13] K. Kaneko. Towards thermodynamics of spatiotemporal chaos. *Prog. Theor. Phys. Suppl.* **99** (1989) 263–287.
- [14] K. Kaneko. Lyapunov analysis and information flow in coupled map lattices. *Physica D* **23** (1986) 436–447.
- [15] N. Parekh, V.R. Kumar and B.D. Kulkarni. Analysis and characterization of complex spatio-temporal patterns in nonlinear reaction-diffusion systems. *Physica A* **224** (1996) 369–381.
- [16] N. Parekh, V.R. Kumar and B.D. Kulkarni. Control of spatiotemporal chaos: a study with an autocatalytic reaction-diffusion system. *Pramana J. of Physics* **48**, 1 (1997) 303–323.
- [17] D. Ruelle. Five turbulent problems. *Physica D* **7** (1983) 40–44.
- [18] P. Manneville. Liapounov exponents for the Kuramoto-Sivashinsky model, in “Macroscopic modeling of turbulent flows”, Springer-Verlag, Berlin. *Lecture Notes in Physics* **230** (1985) 319–326.
- [19] B.R. Parlett. *The symmetric eigenvalue problem*. Prentice-Hall, 1980.
- [20] K. Kaneko. Transition from torus to chaos accompa-

- nied by frequency lockings with symmetry breaking. *Prog. Theor. Phys.* **69**, 5 (1983) 1427.
- [21] K. Kaneko. Period-doubling of kink-antikink patterns, quasiperiodicity in anti-ferro-like structures and spatial intermittency in coupled logistic lattice. *Prog. Theor. Phys.* **72**, 3 (1984) 480–486.
- [22] P.M. Gade and R.E. Amritkar. Spatially periodic orbits in coupled map lattices. *Phys. Rev. E* **47**, 1 (1993) 143–153.
- [23] Q. Zhilin, H. Gang, M. Benkun and T. Gang. Spatiotemporally periodic patterns in symmetrically coupled map lattices. *Phys. Rev. E* **50**, 1 (1994) 163–170.
- [24] R. Carretero-González, D.K. Arrowsmith and F. Valdi. Mode-locking in coupled map lattices. *Physica D* **103** (1997) 381–403.
- [25] R. Kapral, R. Livi, G.-L. Oppo and A. Politi. Dynamics of complex interfaces. *Phys. Rev. E* **49**, 3 (1994) 2009–2022.
- [26] D. Keeler and J.D. Farmer. Robust space-time intermittency and $1/f$ noise. *Physica D* **23** (1986) 413–435.
- [27] C. Beck. Chaotic cascade model for turbulent velocity distribution. *Phys. Rev. E* **49**, 5 (1994) 3641–3652.
- [28] F.H. Willeboordse and K. Kaneko. Pattern dynamics of a coupled map lattice for open flow. *Physica D* **86**, 3 (1995) 428–455.
- [29] R. Carretero-González. *Front propagation and mode-locking in coupled map lattices*. PhD. thesis, Queen Mary and Westfield College, London, U.K., 1997. <http://www.ucl.ac.uk/~ucesca/abstracts.html#abs7>
- [30] V.I. Oseledec. A multiplicative ergodic theorem. Ljapunov characteristic numbers for dynamical systems. *Trans. Moscow Math. Soc.* **19** (1968) 197–231.
- [31] P.J. Davis. *Circulant Matrices*. John Wiley & Sons, 1979.
- [32] R. Bellman. *Introduction to matrix analysis*. McGraw-Hill, 1960.
- [33] S. Vannitsem and C. Nicolis. Error growth dynamics in spatially extended systems. *Int. J. Bifurcation and Chaos* **6**, 12A (1996) 2223–2235.
- [34] S. Barnett. *Matrices: methods and applications*. Oxford University Press, 1990, p. 349.
- [35] G. Mayer-Kress and K. Kaneko. Spatiotemporal chaos and noise. *J. Stat. Phys.* **54**, 5/6 (1989) 1489–1508.
- [36] H. Furstenberg and H. Kesten. Products of random matrices. *Ann. Math. Stat.* **31** (1960) 573–469.
- [37] R.A. Johnson, K.J. Palmer and G.R. Sell. Ergodic properties of linear dynamical systems. *SIAM J. Math. Anal.* **18**, 1 (1987) 1–33.
- [38] N. Parekh, V.R. Kumar and B.D. Kulkarni. Synchronization and control of spatiotemporal chaos using time-series data from local regions. *Chaos* **8**, 1 (1998) To appear.
- [39] M.P. Hassell, H.N. Comins, and R.M. May. Spatial structure and chaos in insect population dynamics. *Nature* **353** (1991) 255–258.
- [40] H.N. Comins, M.P. Hassell and R.M. May. The spatial dynamics of host-parasitoid systems. *J. Anim. Ecology* **61** (1992) 735–748.
- [41] H.B. Wilson and D.A. Rand. Reconstructing the dynamics of unobserved variables in spatially-extended systems. *Proc. R. Soc. Lond. B.* **264** (1997) 625–630.
- [42] P. Rohani and O. Miramontes. Host-parasitoid metapopulations: the consequences of parasitoid aggregation on spatial dynamics and searching efficiency. *Proc. R. Soc. Lond. B.* **260** (1995) 335–342.
- [43] S. Ørstavik, R. Carretero-González and J. Stark. Bounds for interleaving and estimation of intensive measures in spatiotemporal systems from time-series. In preparation.